# The Recognition of Driving Action Based on EEG Signals Using Wavelet-CSP Algorithm

Jinxin Lin[1] , Shunyu Liu[1] , Gan Huang[2] , Zhiguo Zhang[2] and Kai Huang[1]
[1]School of Data and Computer Science, Sun Yat-sen University, Guangzhou, China 510006
[2]School of Biomedical Engineering, Health Science Center, Shenzhen University, Shenzhen, China 518060
Email: {linjx23, liushy39}@mail2.sysu.edu.cn, {huanggan, zgzhang}@szu.edu.cn, huangk36@mail.sysu.edu.cn

***Abstract*—The ability of recognizing driving actions could help building a more advanced driving assitance system, and could even be applied in automated driving to improve the driving safety. In this paper, we investigate the offline recognition of three classes of driving actions (turning left, turning right and braking), based on electroencephalography (EEG) signals. A simulated experiment was conducted to collect EEG data of participants. The proposed algorithm includes Wavelet Analysis and Common Spatial Patterns (CSP), to extract the discriminative features. The classification results were obtained using the Linear Discriminant Analysis (LDA). The results yielded an average single trial classification accuracy of 70.25% for all subjects, showing the discrimination of different actions and the correlation between driving actions and EEG signals.**

***Index Terms*—Driving action recognition; Electroencephalography (EEG); Braincomputer interface (BCI); Common Spatial Patterns (CSP); Wavelet analysis; Linear Discriminant Analysis (LDA)**

## I. Introduction

Automated driving is widely regarded as one of the main technical means to solve traffic safety problems. However, many obstacles still remain on the road to fully automated driving. On March 19th, a self-driving Uber vehicle struck a pedestrian in an accident in the US [1]. The safety driver inside the vehicle was supposed to brake, but he didn't respond. This accident warns us that the safety of automated driving is still a major concern. In the case of non-fully automated driving, such as level 3 or level 4 automated vehicles graded according to the SAE J3016 standard [2], drivers should take over driving in emergency. Drivers may brake, turn left or turn right to avoid accidents. Recognizing these driving actions would enhance the safety of automated driving. Moreover, it could help building a more advanced driver assistance system.

Typically, objective driving data (steering angle, acceleration, etc.) constitutes the main source of driving behavior recognition. Most existing research collect data from in-vehicle sensors to identify various driving behaviors or styles [3], [4]. In [5], In-Vehicle CAN-Bus information was used for classification of driving actions. In prevailing studies, just a few utilize physiological signal to recognize driving behavior. Among various physiological signals, electroencephalography (EEG) can directly reflect the driver's nervous state, with the advantages of non-invasive and high temporal resolution. A two-layer learning method was proposed to recognize driving behavior [6], using EEG data collected in simulated driving experiment. Moreover, we can even predict driving intention by the utilization of slow anticipatory related potentials in EEG. Compared with other methods of driving behavior recognition, it is an incomparable advantage. In [7], the authors researched two types of driving actions (braking and accelerating). By decoding slow cortical potentials, they demonstrated the discrimination between actions, and showed the feasibility of predicting the driver's intension.

Similar to the brain-computer interface (BCI) system based on motor imagery, the physiological basis of driving action recognition is the event-related synchronization (ERS) and desynchronization (ERD) [8], [9]. In the course of performing a driving action, the energy of $\mu$ (8-12 Hz) and $\beta$ (18-30 Hz) rhythms will increase or decrease in the corresponding motor cortex. Therefore, we can distinguish different actions according to the spatial distribution of EEG signals around 8 Hz and 30 Hz.

In order to classify three classes of driving actions, the features of EEG signals should be extracted. But the low signal-to-noise ratio, nonstationarity and randomicity of EEG makes it challenging to develop an efficient algorithm. Currently, the Common Spatial Patterns (CSP) algorithm is widely used for the feature extraction of two-class EEG and the effectiveness of it has been proven [10]. For multi-class problems, One-Versus-One (OVO) and One-Versus-the-Rest (OVR) [11] strategies are often used. CSP has good spatial resolution, but a single CSP algorithm lacks frequency domain information. According to ERD/ERS, by detecting the differences in the $\mu$ and $\beta$ frequency band, different actions could be classified. The Wavelet Analysis [12], as a fast algorithm for time-frequency analysis, effectively compensates for frequency domain defects of CSP.

In this work, we investigate the recognition of driver's actions (turning left, turning right and braking) offline, based on the analysis of EEG signal. We collected subjects' EEG data during the driving action tasks in a simulated experiment. Then we combined the method of Wavelet Analysis and CSP, to extract the features of EEG signals. Finally, the Linear Discriminant Analysis (LDA) [13] was used to classify the three classes of driving actions.

## II. Experiment

We performed a simulated experiment to collect EEG signals while the subjects performed three classes of driving actions.

Three images were displayed in different trials to instruct subjects to turn left, turn right or brake.

### A. Equipments and Subjects

We performed the experiment in the School of Data and Computer Science at Sun Yat-sen University. EEG signal was recorded using 64 Ag/AgCl electrodes arranged in the 10-20 standard, using a Brain Products GmbH BrainAmp Amplifier and an EasyCAP EEG cap. The sampling rate was 1000 Hz. And we used Logitech G27 racing steering wheel and pedal to perform driving actions.

Ten healthy subjects (four female, aged between 20-25 years) participated in our experiment. The average driving experience of all subjects was more than two years. They all signed informed consent and were paid for the experiment.

### B. Experimental Design

Each subject participated in one session recorded on a single day. Each session consisted of 5 runs with 60 trials for each one, recorded consecutively with short breaks between two runs. There are 300 trials taken together, and 100 trials for each class of actions. The first 3 runs of each subject's data were used for training and the last 2 runs for testing.

The course of a single trial is shown in Fig. 1. Each trial started with 2 s of white screen. At $t = 2$ s, a black cross appeared in the middle of screen for 0.5 s. An image (turn left sign, turn right sign or stop sign, shown in Fig. 2) was displayed from $t =$ 3-10 s. The subjects were asked to perform corresponding driving actions according to the type of the image, as soon as they saw it. At $t = 10$ s, a break with 1 s was followed. The experiment scene is shown in Fig. 3.


Figure 1: The course of a single trial


(a) Turn left sign. (b) Stop sign. (c) Turn right sign.

Figure 2: Images displayed on the screen.

## III. Methodology

The framework of the proposed algorithm is shown in Fig. 4. We preprocessed the raw data with a 50 Hz notch filter and a 0.5-100 Hz 4th-order bandpass Butterworth filter. Then a Wavelet-CSP (W-CSP) algorithm, using Discrete Wavelet Transform

Figure 3: Driving action experiment scene

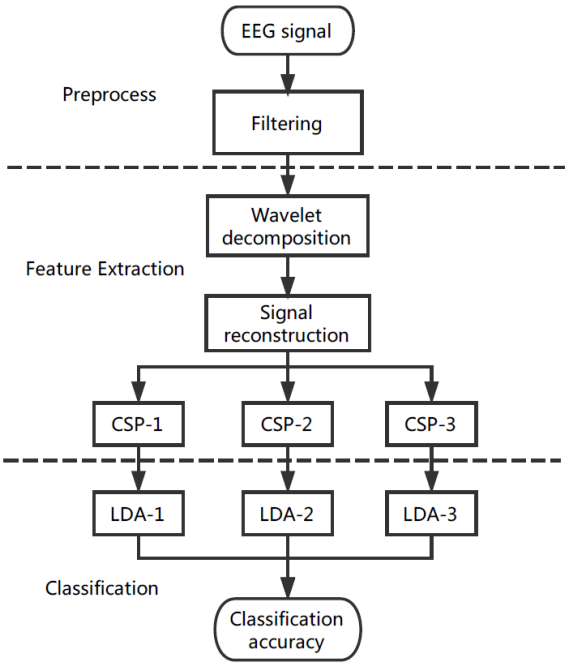


Figure 4: Proposed algorithm for recognition of driving actions

(DWT) before applying CSP with OVO strategy, was used to extract the discriminative features. In the three binary-class subproblems, three CSP projection matrices were calculated. Three binary-class LDA classifiers were trained to classify these features, and the final classification results were obtained by voting.

### A. Discrete Wavelet Transform

In Discrete Wavelet Transform, wavelets are prototype functions, similar to bandpass filters. By using DWT, low frequency component shows fine frequency resolution, while fine temporal resolution obtained at high frequency component. The sampled signal $x[n]$ can be decomposed by DWT as follows [14]:

$$x[n] = \sum_{i=1}^{L} D_i + A_L = D_1 + D_2 + \cdots + D_L + A_L \quad (1)$$

where $L$ is the maximum number of decomposition levels, $D_i$ is the detail component, and $A_L$ is the approximation component. If $F_s$ denotes the sampling rate, according to the Sampling theorem, the maxinum effective frequency is $F_s/2$. The sub-frequency bands of $x[n]$ are: $D_1(F_s/2^2,\ F_s/2)$, $D_2(F_s/2^3,\ F_s/2^2)$, $\ldots$ , $D_L(F_s/2^{L+1},\ F_s/2^L)$, $A_L(0,\ F_s/2^{L+1})$.

The raw signals were downsampled to 500 Hz, and a five-layer wavelet decomposition for Daubechies wavelet of order 4 (db4) followed. The sub-frequency bands after DWT are: $D_1$ (125-250 Hz), $D_2$ (62.5-125 Hz), $D_3$ (31.25-62.5 Hz), $D_4$ (15.625-31.25 Hz), $D_5$ (7.8125-15.625 Hz), $A_5$ (0-7.8125 Hz). The frequency bands of $D_4$ and $D_5$ contains 8-30 Hz, therefore, the signals were reconstructed using wavelet reconstruction with the coefficients $cD_4$ and $cD_5$.

### *B. Common Spatial Pattern*

The CSP algorithm is based on the simultaneous diagonalization of two covariance matrices [15], and can maximize the differences between the two classes of signals. Suppose that the single trial EEG data is $X$ of size $N * S$, where $N$ denotes the number of channels, and $S$ denotes the number of samples for each channel. The normalized spatial covariance of the trial is:

$$C = \frac{XX^T}{trace(XX^T)} \tag{2}$$

where $X^T$ represents the the transpose of matrix $X$, and $trace(\cdot)$ denotes the sum of diagonal elements. Then the sum of covariance matrices for the two classes is calculated:

$$C_1 = \sum_{i \in I_1} C_i, \quad C_2 = \sum_{i \in I_2} C_i \tag{3}$$

where $i \in I_{1,2}$ denotes that the i-th trial belongs to class 1 or 2. Perform the eigenvalue decomposition on the sum of $C_1$ and $C_2$, we get:

$$C_c = C_1 + C_2 = U_c \lambda U_c^T \tag{4}$$

where $U_c$ denotes the matrix of eigenvectors, and $\lambda$ denotes the diagonal matrix of eigenvalues. Then construct the whitening matrix:

$$P = \sqrt{\lambda^{-1}} U_c^T \tag{5}$$

And whiten the two covariance matrices:

$$S_1 = PC_1P^T, \quad S_2 = PC_2P^T \tag{6}$$

Because the two covariance matrices are simultaneously diagonalized, $S_1$ and $S_2$ have the same eigenvectors:

$$S_1 = U\lambda_1 U^T, \quad S_2 = U\lambda_2 U^T \tag{7}$$

and corresponding eigenvalues satisfy:

$$\lambda_1 + \lambda_2 = I \tag{8}$$

where $I$ denotes the identity matrix. Therefore, the eigenvalue of one class of signals is the largest, while that of the other class is the smallest. Then we obtain the CSP projection matrix:

$$W = U^T P \tag{9}$$

And the spatially filtered EEG signal is:

$$Z = WX \tag{10}$$

In order to extract the features, consider the signals $Z_p(p = 1, 2, \ldots, 2k)$ with the largest $k$ eigenvalues in $S_1$ and $S_2$. Thus by selecting the first and last $k$ rows of $Z$, we get the feature vectors [10]:

$$f_p = \log(\frac{var(Z_p)}{\sum_{i=1}^{2k} var(Z_i)}) \tag{11}$$

where $var(\cdot)$ represents the variance of signal.

## IV. Results and Discussions

20 channels around C3, Cz and C4 (FC5, FC3, FC1, FC2, FC4, FC6, C5, C3, C1, Cz, C2, C4, C6, CP5, CP3, CP1, CPz, CP2, CP4, CP6) were selected from all datasets for the analysis. We firstly dowmsampled the raw signals to 500 Hz. After preprocessing the raw data with notch and bandpass filters, we decomposed all the signals with DWT. Then the detail components $D4$ and $D5$ were used to reconstruct the EEG signals. The topographical maps of three classes of signals after DWT from subject 4 are shown in Fig. 5. It shows that ERD/ERS appears in the corresponding area of the motor cortex. Taking braking as an example, ERD appears in the area around electrode Cz. This reflects the correlation between driving actions and EEG signals.

Before CSP spatial filtering, 20 channels and 2 sub-frequency components were utilized to create 40 new channels. Therefore, the size of single trial became $40 * Samples$. By applying CSP algorithm, the spatially filtered EEG signals were obtained. We selected the first three and the last three rows to form the discriminative features. Fig. 6 depicts the distributions of the first and last dimension of features in the three binary-class subproblems. Finally, we got the classification accuracy using LDA.

For comparison, we used the conventional CSP algorithm to extract the features and calculated the performance. The downsampled signals were preprocessed with a 8-30 Hz 4th-order bandpass filter before CSP. And LDA was also utilized to get the classification results.

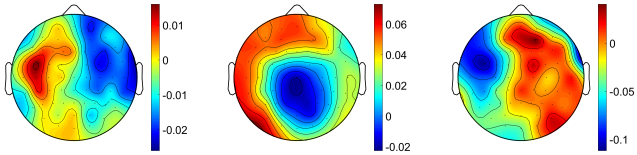


(a) Turning left (b) Braking (c) Turing right

Figure 5: The topographical maps of ERD/ERS. Signals of three classes of actions were averaged over the corresponding trials, and the segment of 3.5-4 s was selected to draw the maps.

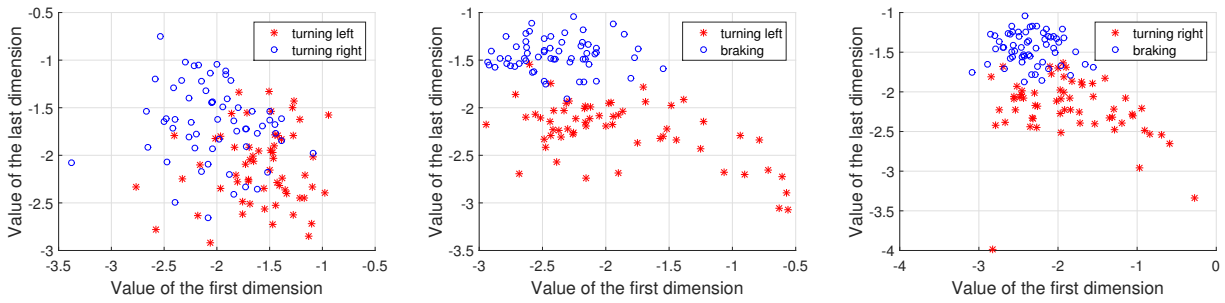


(a) Features of turning left and turning right (b) Features of turning left and braking (c) Features of turning right and braking

Figure 6: Distributions of the first and last dimension of features obtained by W-CSP.

### A. *The Best Time Segment Selection*

To get the best classification results, different time segments for analysis were selected to apply CSP. We applied a 3 s sliding window in the segment of 2-10 s, with a 0.5 s step. Fig. 7 shows the classification accuracy of subject 4. The accuracy is relatively low at the begining, and reaches the highest (77.50%) in the segment of 4.5-7.5 s. Then the accuracy gradually decreases. The best time segment varies with the subject, thus we selected the most suitable one for each dataset.

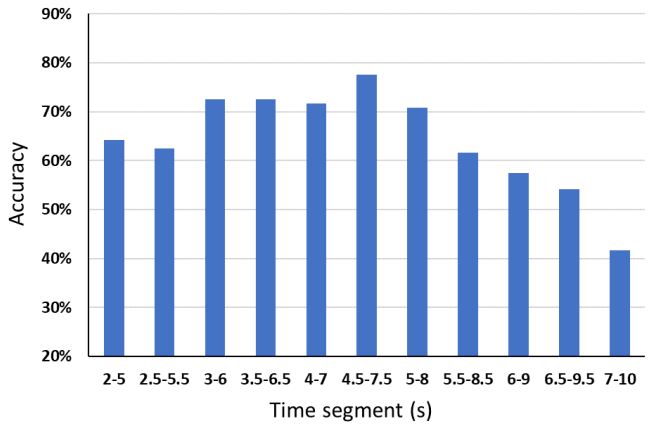


Figure 7: The classification accuracy of different time segments (subject 4).

### B. *Classification Results*

The best time segment of each train set was selected for the calculation of the CSP projection matrix and the LDA training. Then the classification accuracy was obtained on the test set.

In Table I, the classification accuracy of W-CSP and CSP are concluded. The average accuracy is 70.25% for W-CSP, and 68.08% for CSP. It shows that our algorithm outperforms the conventional CSP method. And the standard deviation of W-CSP (5.82) is less than that of CSP (6.34), showing that the stability of our algorithm is better. In addition, the results indicate significant individual differences in driving action recognition, which is inevitable in EEG-based BCI systems.

Table I: Performance of Driving Action Recognition

| Subject | Accuracy(%) | |
|---|---|---|
| | W-CSP | CSP |
| 1 | 70.00 | 74.17 |
| 2 | 70.83 | 67.50 |
| 3 | 60.00 | 60.83 |
| 4 | 77.50 | 73.33 |
| 5 | 77.50 | 77.50 |
| 6 | 60.00 | 56.67 |
| 7 | 73.33 | 72.50 |
| 8 | 72.50 | 63.33 |
| 9 | 68.33 | 70.83 |
| 10 | 72.50 | 64.17 |
| Average | 70.25 | 68.08 |
| Std | 5.82 | 6.34 |

## V. Conclusion and Future Works

The purpose of this study was to recognize three classes of driving actions in an offline analysis. The proposed Wavelet-CSP algorithm combined DWT and CSP method, providing discriminative features to classify driving actions. And LDA was used to classify the features. The average classification accuracy was 70.25% for 10 subjects, at the best time segment for each subject. The results indicated that our algorithm had a higher classification accuracy than the conventional CSP algorithm.

In future works, we plan to combine this study with the detection of anticipatory brain potentials, to predict which action the driver is to perform. Online algorithm should be researched to assess the real-time performance of driving action detection and classification. The technology of predicting the driver's action can be use in driving assistance system or automated cars, to improve driving safety.

## Acknowledgment

The authors would like to thank the reviewers for their valuable comments of this paper. This work is supported partly by the funding from Science and Technology Innovation Committee of Shenzhen Municipality under Grant Number J20180129.

## REFERENCES


[1] D. Wakabayashi, "Self-Driving Uber Car Kills Pedestrian in Arizona, Where Robots Roam," https://www.nytimes.com/2018/03/19/technology/uber-driverless-fatality.html, [Accessed March. 19, 2018].

[2] S. International, "Taxonomy and definitions for terms related to driving automation systems for on-road motor vehicles," 2016.

[3] M. Jensen, J. Wagner, and K. Alexander, "Analysis of in-vehicle driver behaviour data for improved safety," *International journal of vehicle safety*, vol. 5, no. 3, pp. 197–212, 2011.

[4] M. V. Ly, S. Martin, and M. M. Trivedi, "Driver classification and driving style recognition using inertial sensors," in *2013 IEEE Intelligent Vehicles Symposium (IV)*, 2013, pp. 1040–1045.

[5] S. Choi, J. Kim, D. Kwak, P. Angkititrakul, and J. H. Hansen, "Analysis and classification of driver behavior using in-vehicle can-bus information," in *Biennial Workshop on DSP for In-Vehicle and Mobile Systems*, 2007, pp. 17–19.

[6] L. Yang, R. Ma, H. M. Zhang, W. Guan, and S. Jiang, "Driving behavior recognition using EEG data from a simulated car-following experiment," *Accident Analysis & Prevention*, vol. 116, pp. 30–40, 2018.

[7] Z. Khaliliardali, R. Chavarriaga, L. A. Gheorghe, and J. del R Millán, "Action prediction based on anticipatory brain potentials during simulated driving," *Journal of neural engineering*, vol. 12, no. 6, p. 066006, 2015.

[8] G. Pfurtscheller and A. Aranibar, "Evaluation of event-related desynchronization (ERD) preceding and following voluntary self-paced movement," *Clinical Neurophysiology*, vol. 46, no. 2, pp. 138–146, 1979.

[9] G. Pfurtscheller and C. Neuper, "Event-related synchronization of mu rhythm in the EEG over the cortical hand area in man," *Neuroscience letters*, vol. 174, no. 1, pp. 93–96, 1994.

[10] H. Ramoser, J. Muller-Gerking, and G. Pfurtscheller, "Optimal spatial filtering of single trial EEG during imagined hand movement," *IEEE transactions on rehabilitation engineering*, vol. 8, no. 4, pp. 441–446, 2000.

[11] W. Wu, X. Gao, and S. Gao, "One-Versus-the-Rest(OVR) Algorithm: An Extension of Common Spatial Patterns(CSP) Algorithm to Multi-class Case," in *2005 IEEE Engineering in Medicine and Biology 27th Annual Conference*, 2005, pp. 2387–2390.

[12] L. Qin and B. He, "A wavelet-based time–frequency analysis approach for classification of motor imagery for brain–computer interface applications," *Journal of neural engineering*, vol. 2, no. 4, p. 65, 2005.

[13] C. M. Bishop, *Pattern Recognition and Machine Learning*. Springer-Verlag New York, Inc., 2006.

[14] D. Cvetkovic, E. D. Übeyli, and I. Cosic, "Wavelet transform feature extraction from human PPG, ECG, and EEG signal responses to ELF PEMF exposures: A pilot study," *Digital signal processing*, vol. 18, no. 5, pp. 861–874, 2008.

[15] K. Fukunaga, *Introduction to statistical pattern recognition*. Academic press, 2013.